JACS
JOURNAL OF THE AMERICAN CHEMICAL SOCIETY

ARTICLE

pubs.acs.org/JACS

# Structural Basis of Telomeric RNA Quadruplex−Acridine Ligand Recognition

Gavin W. Collie, Silvia Sparapani, Gary N. Parkinson, and Stephen Neidle*

CRUK Biomolecular Structure Group, The School of Pharmacy, University of London 29-39 Brunswick Square, London WC1N 1AX, United Kingdom

**ABSTRACT:** Human telomeric DNA is now known to be transcribed into noncoding RNA sequences, termed TERRA. These sequences, which are believed to play roles in the regulation of telomere function, can form higher-order quadruplex structures and may themselves be the target of therapeutic intervention. The crystal structure of a TERRA quadruplex−acridine small-molecule complex at a resolution of 2.60 Å, is reported here and contrasts remarkably with the structure of the analogous DNA quadruplex complex. The bimolecular RNA complex has a parallel-stranded topology with propeller-like UUA loops. These loops are held in particular conformations by multiple hydrogen bonds involving the O2′ hydroxyl groups of the ribonucleotide sugars and play an active role in binding the acridine molecules to the RNA quadruplex. By contrast, the analogous DNA quadruplex complex has simpler 1:1 acridine binding, with no loop involvement. There are significant loop conformational changes in the RNA quadruplex compared to the native TERRA quadruplex (Collie, G. W.; Haider, S. M.; Neidle, S.; Parkinson, G. N. *Nucleic Acids Res.* **2010**, *38*, 5569−5580), which have implications for the future design of small molecules targeting TERRA quadruplexes, and RNA quadruplexes more generally.

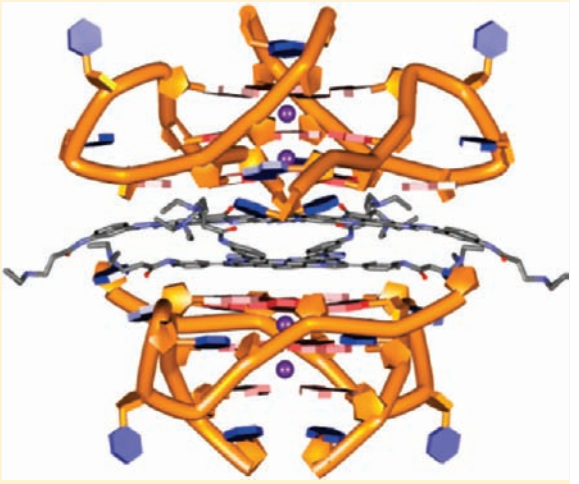

## INTRODUCTION

The DNA component of telomeres in eukaryotic organisms, comprising tandem repeats of simple guanine-rich sequences,[1] has long been assumed to be transcriptionally silent. In humans and other mammals this repeat is TTAGGG. The recent findings[2,3] that the C-rich strand of telomeric DNA is transcribed into lengths of telomeric RNA (termed TERRA) were therefore totally unexpected. TERRA is composed of tandem rUUAGGG repeats that vary between 100 and 1000 bp in length and may be involved in a number of key cellular processes,[4,5] including chromatin regulation and remodelling. It has also been demonstrated that TERRA sequences are potent and direct inhibitors (and thus negative regulators) of telomerase function.[6] Several TERRA-interacting proteins have been identified, notably the telomeric duplex DNA binding proteins TRF1 and TRF2, pointing to a significant role of TERRA in more general chromosome biology.[7−9] The POT1 protein contains an OB fold, which binds to the single-stranded overhang repeats at the terminus of telomeric DNA and is unable to bind to TERRA.[10]

TERRA repeat sequences show a high propensity to form stable compact structures in vitro, analogous to the behavior of the equivalent G-rich telomeric DNA sequences[11] and consistent with the formation of G-quartets as the packing motif. Solution studies on short (comprising two and four telomeric repeats) TERRA sequences have shown that these readily form highly stable G-quadruplex structures in both sodium and potassium ion containing solution.[12,13] NMR analysis[13,14] of the two-repeat 12-mer sequence rUAGGGUUAGGGU has shown that this forms a highly stable parallel-stranded intermolecular bimolecular quadruplex, with the topology and propeller loop arrangement that has been previously observed for telomeric DNA quadruplexes in the crystalline state.[15] A subsequent crystal structure of the same sequence[16] has found the same topology and has shown that the presence of the 2′ hydroxyl groups, together with the preference of the ribosugars for a C3′-*endo* pucker, plays a significant role in stabilizing the parallel arrangement. This consistency between crystal and solution topologies is in striking contrast to the situation with telomeric DNA quadruplexes, where there is marked topological variability depending on the environmental conditions.[14]

The stabilization of telomeric DNA quadruplex structures with small-molecule ligands can result in the inhibition of the activity of the telomere-maintenance enzyme telomerase,[17] whose expression is up-regulated in the majority of human cancer cells types. A large number of such ligands have been characterized,[18] and several have been used to demonstrate that telomerase inhibition in cancer cells can result in selective inhibition of cell growth, and indeed in antitumor activity in vivo.[19,20] The structures of several quadruplex DNA complexed with acridine-based ligands have been determined by

**Received:** November 10, 2010
**Published:** February 3, 2011





dx.doi.org/10.1021/ja109767y | *J. Am. Chem. Soc.* 2011, 133, 2721–2728

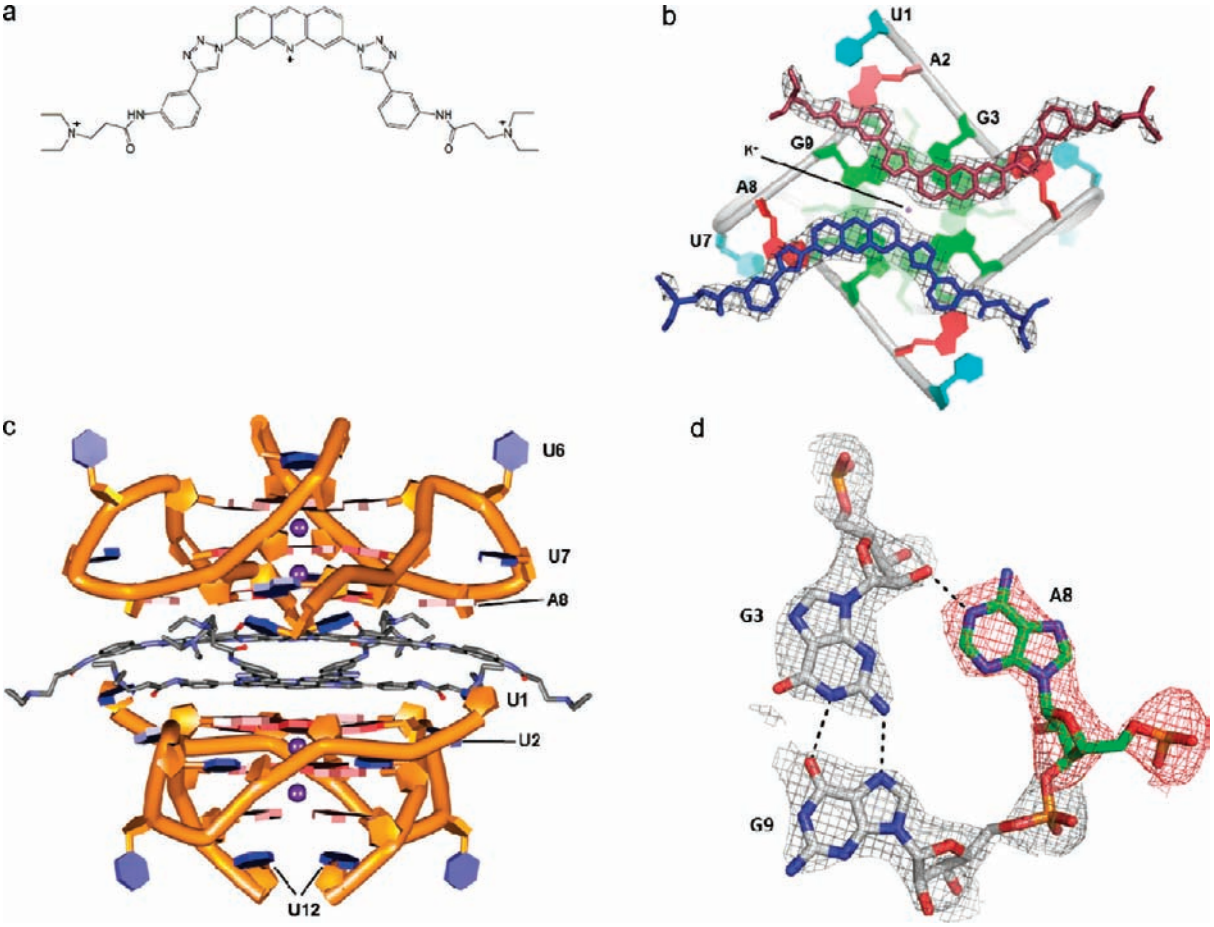


**Figure 1.** (a) Chemical structure of the acridine molecule *N*,*N*′-((1,1′-(acridine-3,6-diyl)bis(1*H*-1,2,3-triazole-4,1-diyl))bis(3,1-phenylene))bis-(2-(diethylamino)acetamide). (b) View of the crystal structure onto the plane of a terminal G-quartet in the complex, showing two stacked and side-by-side acridine molecules. (c) Schematic view of two quadruplexes in cartoon representation of the RNA quadruplex complex, with backbones colored orange and showing the two layers of acridine molecules sandwiched between them. The potassium ions are shown as small mauve spheres and were located midway between the G-quartet planes. (d) $F_o-F_c$ omit electron density map calculated using the RNA model minus residue A8 (red mesh at 1.5 $\sigma$ level). The gray mesh (1.5 $\sigma$ level) shows the electron density from a $2F_o-F_c$ map calculated using the entire RNA model. Carbon atoms of G3 and G9 are colored white, and those of A8 are colored green. Black dashed lines represent intramolecular hydrogen bonding.

crystallography[21,22] and NMR methods,[23] and these have facilitated rationalizations of the biophysical and biological data for these compounds.[21]

These and other telomerase and telomere-targeting ligands have been designed and developed to interact exclusively with telomeric DNA quadruplex structures. The emerging pivotal roles of TERRA in telomere biology suggest that ligands with high affinity and selectivity to TERRA G-quadruplexes may be of therapeutic use. Biophysical data on a number of ligands has shown that selective binding between RNA and DNA telomeric quadruplexes is achievable.[24−26]

Potential RNA G-quadruplex-forming sequences may be encoded elsewhere in genomes other than at telomeres. They have been identified in the 5′ untranslated regions of a number of eukaryotic and prokaryotic genes,[27−29] pointing to a regulatory role of such folded RNA structures in translational inhibition of gene expression.[30−35] Translational inhibition may be enhanced by binding a small molecule to a 5′-UTR quadruplex in order to enhance its stability, as has been demonstrated for the human NRAS gene.[36] Quadruplex-binding ligands can also inhibit dicer quadruplex RNA processes.[37] There is as yet very little structural information on these RNA quadruplexes, but circular dichroism data suggests that a parallel fold is common to many of these structures, together with increased stability for RNA quadruplexes over the equivalent DNA structures.[24,38−40]

We present here the crystal structure of a TERRA RNA quadruplex complexed with an acridine ligand extended in length by triazole-based click chemistry. This ligand is symmetrically substituted at the 3- and 6-positions with triazole-phenyl-diethylamine side chains (Figure 1a) and was originally designed to bind optimally to telomeric DNA quadruplexes.[41] It shows selectivity over several other DNA quadruplexes, notably those found in the promoter sequence of the *c-kit* gene. Crystal structures of several ligand−DNA quadruplex complexes,[21,22,42] together with theoretical calculations,[16,41] have shown that the ligand planar surfaces are stabilized by interaction with a terminal G-quartet surface and that the loops can play a secondary role by interacting with substituents. In general loop conformations are highly conserved[43] in native telomeric DNA quadruplexes, whereas ligands can trap particular conformations. The RNA quadruplex complex crystal structure presented here reveals a pattern of active loop involvement in ligand recognition that involves several major RNA-dependent changes in loop conformation, which have relevance to the future design of ligands


dx.doi.org/10.1021/ja109767y |*J. Am. Chem. Soc.* 2011, 133, 2721–2728

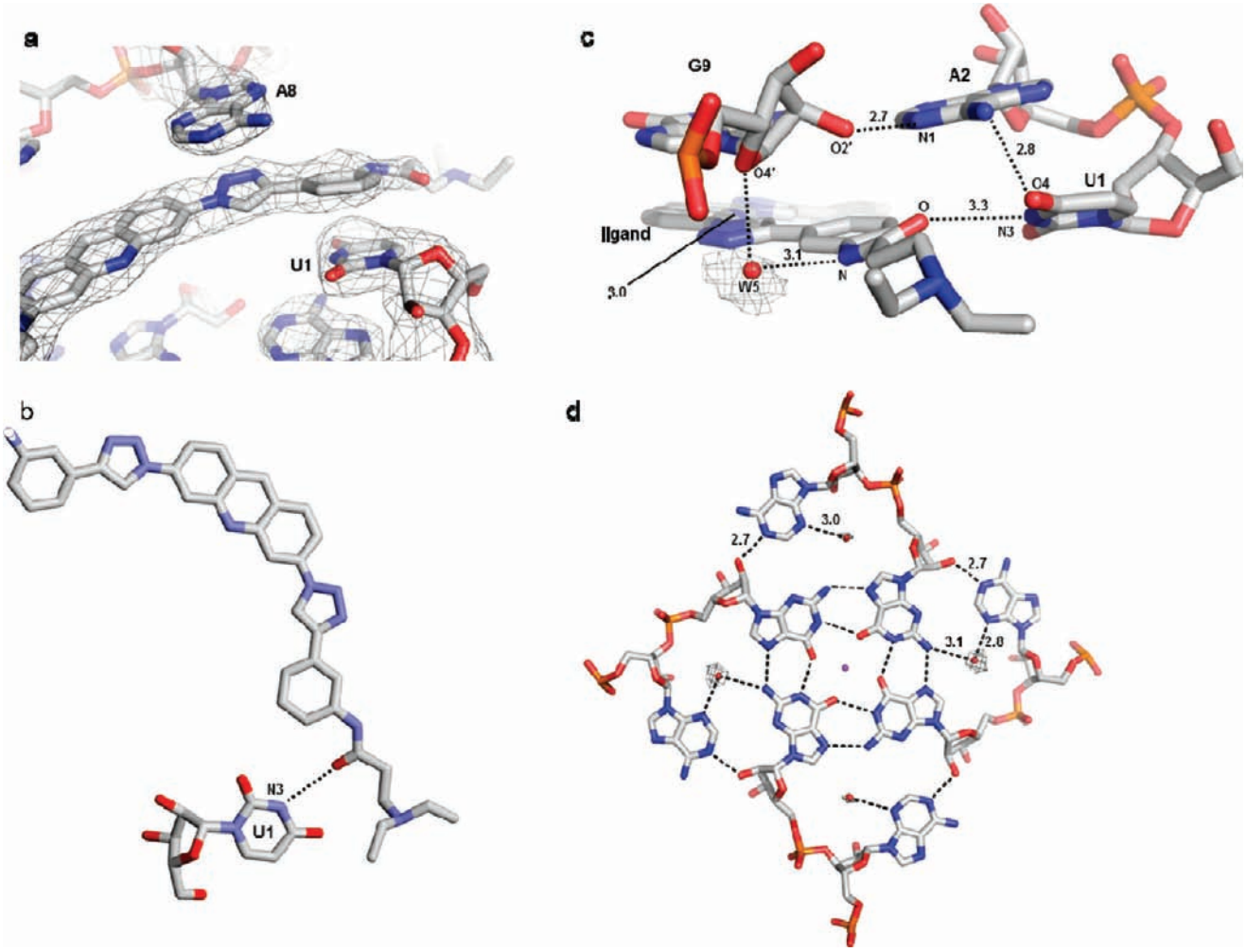


**Figure 2.** (a) $2F_o-F_c$ electron density map, contoured at 1.0 $\sigma$, showing the triazole and terminal phenyl rings of an acridine molecule intercalatively stacked between an adenine and a uracil base. (b) View of the hydrogen-bond arrangement between the amide oxygen atom at one end of a ligand molecule and uracil U1. (c) The hydrogen-bonding arrangement involving the amide group at one end of the ligand, a water molecule, and nucleosides U1, A2, and G9, notably the interaction involving the O2′ atom of G9. The electron density of water molecules is shown taken from a $2F_o-F_c$ map, contoured at 0.5 $\sigma$. (d) A view of the G4A4 octet of bases and the hydrogen bonds between them. The electron density of water molecules is shown contoured at 0.5 $\sigma$.

targeting various categories of defined DNA and RNA quadruplexes.

## RESULTS

**Overall Arrangement of the Ligand Complex.** The crystallographic asymmetric unit contains one human telomeric RNA strand of the sequence r(UAGGGUUAGGGU) and one triazole-acridine ligand molecule. The biological unit is formed by a crystallographic twofold rotation axis and comprises a bimolecular G-quadruplex formed from two strands of the RNA sequence, complexed to two molecules of the ligand (Figure 1a). The quadruplex is parallel-stranded with linking UUA propeller-like chain-reversal loops. The two triazole-acridine ligand molecules are stacked side-by-side onto a single terminal 5′ G-quartet face (Figure 1b). Two complete intermolecular quadruplexes are arranged in the crystal structure in a 5′ to 5′ manner, with a sandwich of two layers of ligand molecules between them (Figure 1, parts b and c). There are very few direct RNA−ligand hydrogen-bond contacts, the primary mode of interaction being $\pi-\pi$ stacking. The central nitrogen atoms of the acridine rings are orientated away from the center of the quadruplex, such that the two ligand molecules comprising the dimer on each quartet face are arranged in a laterally displaced back-to-back manner (Figure 1b) across the crystallographic twofold axis and around the central potassium ion channel. There are no direct contacts between the two coplanar ligand molecules.

In addition to the nonpolar surface provided by the 5′ G-quartet for $\pi$-stacking, the adenine residues of the propeller-like loops are flipped up toward the ligands, orientating themselves within the plane of the 5′ quartet and providing a platform for the triazole rings of the ligand (Figure 2a). The adenines are thus participants in a novel pseudo-four-fold all-purine G4A4 octet arrangement comprising four guanines from the G-quartet together with the four loop adenines (Figure 2d), which significantly increases the surface area available to the ligand for $\pi$-stacking interactions. The majority of the ligand aromatic groups are positioned directly over the purines, with only one phenyl group not being positioned over the purine-octet binding platform (Figure 1b). Both of the highly polar triazole rings are


dx.doi.org/10.1021/ja109767y |J. Am. Chem. Soc. 2011, 133, 2721–2728

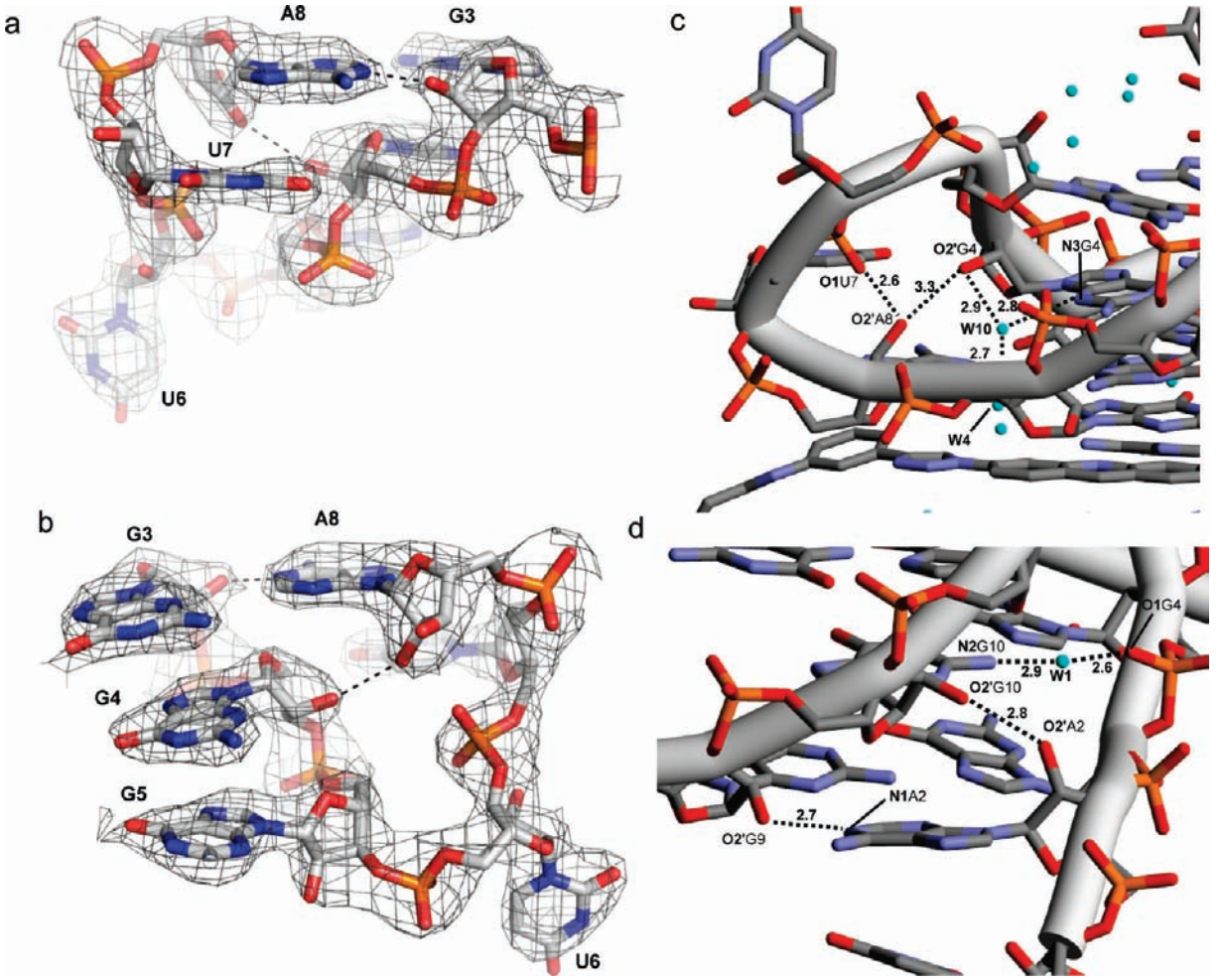


**Figure 3.** (a) $2F_o-F_c$ electron density map of a loop, contoured at 1.0 $\sigma$, showing the stacking between U7 and A8 together with the G4...A8 O2′−O2′ and A8−G4 N1−O2′ hydrogen bond. (b) $2F_o-F_c$ electron density map of the internal loop, contoured at 1.0 $\sigma$, showing the G4−A8 O2′−O2′ hydrogen bond. (c and d) Detailed views of the hydrogen bonding in the internal and terminal loops, respectively.

stacked over purines; one end of the ligand is held in a pseudointercalated manner (Figure 2a), stacked effectively between one adenine and a terminal uracil base. The overlap between triazoles and adenine/uracil is minimal at the other end of the ligand, but here instead there are several hydrogen-bond contacts. The involvement of the loop adenine bases in the G4A4 octet is a consequence of the hydrogen bonding in the loops (described in detail below).

The ligand itself is involved in few hydrogen-bonded contacts with the RNA. There is a weak hydrogen bond (3.3 Å) between the amide carbonyl group at the minimal stacked end of the ligand side chain and the N3 nitrogen of the 5′ terminal uracil residue (Figure 2b). A water molecule mediates with a pair of strong hydrogen bonds between the amide nitrogen atom and the O4′ ribose sugar ring atom of an adjacent guanosine (Figure 2c). The arrangement in this region is tightly ordered since there is also a hydrogen bond between the O2′ of this guanosine and the 5′ adenine (confirmed by an omit map, shown in Figure 1d); this base also hydrogen bonds to the neighboring terminal uracil. The ligand, despite having a potentially high degree of intrinsic conformational flexibility, adopts a predominantly planar conformation, with only a slight deviation from planarity occurring at the triazole-phenyl link, where the ligand side chains curve up toward the 5′ face of a symmetry-related biological unit. This planar arrangement is due in large part to the high degree of overlap between the aromatic groups of the ligand and the purine octet.

**The Purine Octets Involve Water Molecule Bridges.** The core of the G4A4 octet is the 5′ G-quartet. The four adenines surrounding it and in the same plane (Figure 2d) originate from the UUA loop (loop 1) and the 5′ terminal UA sequence, which may be considered to be an incomplete second trinucleotide loop (loop 2). The loop 1 adenine is strongly hydrogen-bonded via base atom N1 to the 2′ hydroxyl group of the adjacent guanosine, and in addition there is a water-mediated pair of hydrogen bonds linking the adenine N3 atom and the N2 of this guanine. This pattern is repeated across the other side of the G-quartet as a consequence of the crystallographic twofold symmetry. The two 5′ adenines form the final components of the octet. These are involved in similar interactions to the first adenine pair, notably a strong hydrogen bond to a guanosine 2′ hydroxyl group and a hydrogen bond to a water molecule that similarly sits between the adenine and the adjacent guanine. The four adenine bases are slightly tilted out of the mean octet plane, by ∼6−8°.

**Loop Conformations.** The UUA loop and the incomplete 5′-UA loop are both held in particular orientations by a combination of base···base stacking and intraloop hydrogen bonding, some of which is RNA-specific. The UUA loop (Figure 3, parts a and b)


dx.doi.org/10.1021/ja109767y |J. Am. Chem. Soc. 2011, 133, 2721–2728

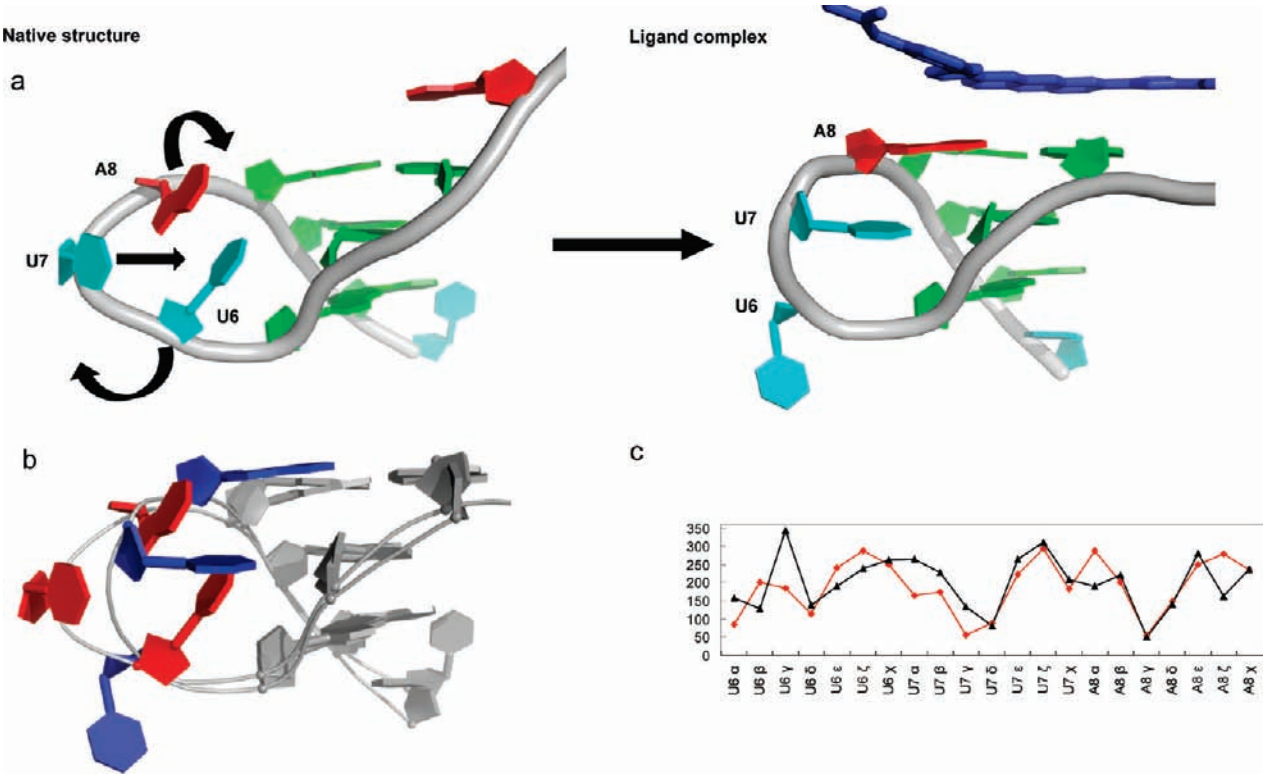


**Figure 4.** (a) Schematic showing the native and ligand-bound loops in cartoon form, highlighting the conformational changes between them. The arrows indicate those bases that have altered glycosidic angles. (b) Superposition of the native (red) and ligand-bound (blue) loops. (c) Plot of the loop backbone angles, showing the native loop values in red and the ligand-bound ones in black.

has the 5′ U6 swung out from the loop, and the adjacent bases, U7 and A8, are approximately parallel yet poorly stacked on each other at a separation of >3.6 Å. There are several cross-loop hydrogen bonds that serve to stabilize the loop conformation (Figure 3c). The A8 2′ hydroxyl group is hydrogen-bonded with a phosphate oxygen atom from the adjacent U. It also hydrogen bonds, more weakly, with the 2′ hydroxyl group from residue G4. This hydroxyl group is also the terminus of a two-water molecule bridge to the N3 atom of G4 and N3 of A8. The incomplete 5′-UA loop has three short cross-loop hydrogen bonds involving the two 2′ hydroxyl groups, from A2 and G10, and between O2′ of G9 and N1 base atom of A2 (Figure 3d). A water molecule is bridging, using two hydrogen bonds, between the N2 of G10 and a G4 phosphate oxygen atom.

**Loop Conformational Reorganization.** Comparison of the conformational angles for the loop residues with those of the native RNA quadruplex[16] highlights the significant reorganization in loop structure that has taken place on ligand binding. The orientations of all three bases in the native loop, U6, U7, and A8, which are almost perpendicular to the G-quartet planes in the native structure, are changed so that U7 and A8 become aligned with the G-quartets (Figure 4, parts a and b). In particular A8 becomes part of the extended G4A4 octet so that it can stack with part of the ligand. Examination of the individual backbone torsion angles (Figure 4c) shows that the changes needed to produce the ligand binding site involving the A8 platform are not uniform along the UUA loop sequence. The angle $\gamma$ in U6 increases by ca. 140°, whereas few other angles in this nucleotide are significantly altered. Angle $\alpha$ increases in U7 by ca. 90°, and angles $\beta$ and $\gamma$ increase by lesser amounts, up to 60°. There are two significant changes in A8 in the ligand-complexed structure, decreases in $\alpha$ and $\zeta$ of ca. 75°. It is notable that the glycosidic angles have closely similar values in the native and ligand complexes, suggesting that this feature of RNA quadruplexes remains constant, along with sugar pucker.

## DISCUSSION

The topology of telomeric RNA quadruplexes is rather rigid and appears to remain in the all-parallel fold under a variety of environmental conditions, in striking contrast to the polymorphism observed for telomeric DNA quadruplexes.[12−16] This has been ascribed to the structure-stabilizing role of the 2′ hydroxyl substituents in RNA quadruplexes.[13,16] It is thus at first sight paradoxical that these groups also play a key role in changing the UUA loop conformation in the present ligand−quadruplex complex. However, it is also apparent from this structure that the loop structural reorganization is driven by the requirement to maximize interactions with the ligand, especially with its planar component. Hence, the G4A4 purine octet motif is stabilized both by stacking interactions with the planar ligand substituents and by a series of pivotal hydrogen bonds with 2′ hydroxyl groups (Figure 2, parts c and d). Such an arrangement is not obviously available to a DNA quadruplex, although a A2G4 hexad has previously been observed in a DNA quadruplex−ligand complex.[42] So although there are no direct interactions with the ligand from the 2′ hydroxyl groups in the present structure, RNA structural selectivity has been achieved in a more indirect manner.

The observation here of induced ligand modification of loop conformation reinforces and extends to RNA quadruplexes the


dx.doi.org/10.1021/ja109767y |J. Am. Chem. Soc. 2011, 133, 2721–2728

earlier conclusions from an analysis of their observed conformations[43] that rational design and optimization of such compounds cannot be based on structural knowledge of native quadruplexes alone, even though in all the crystal structures reported to date the loops retain their overall propeller topology. The 12-mer DNA quadruplex−BRACO-19 ligand complex[21] shows loop modifications consequent to ligand binding that optimize nonbonded interactions with the substituent side chains of this particular ligand. The 12-mer and 23-mer DNA telomeric quadruplexes with a bound naphthalene diimide ligand[42] and the 12-mer with bound porphyrin ligand TMPyP4[44] also show loop conformations differing from those in the native crystal structures.[15] The loop conformations in most of these DNA quadruplex complexes are stabilized by stacking interactions with ligand molecules on the exterior of the quadruplexes, separate from the G-quartet interactions, and are thus not involved in the recognition of tightly bound ligand molecules. In no instance is a DNA loop stabilized by internal hydrogen bonding, a key difference between these and the RNA loops in the present structure. This has been confirmed by a medium-resolution (3.20 Å) crystal structure of the analogous DNA bimolecular quadruplex cocrystallized with the same acridine ligand. The overall structure of this quadruplex complex is closely similar to that observed in previous crystal structures,[21,42,43] with a single (disordered) ligand molecule bound on a G-quartet face (Figure 5) and the complex having 1:1 stoichiometry, in contrast to the 2:1 observed in the present RNA complex. The acridine core in the DNA complex is positioned over the central ion channel of the quadruplex, as seen in previous acridine quadruplex structures,[21,22] contrasting with the offset positioning in the RNA complex. There are no loop−acridine contacts in the DNA complex and no G4A4 octet. We conclude that these differences between the DNA and RNA complexes are due to the presence of the 2′ hydroxyl groups in the RNA and their active involvement in UUA loop conformation remodeling and ligand recognition.

The recent demonstration of the presence of discrete TERRA RNA quadruplexes in cells,[45] together with the finding that it is a natural inhibitor of the telomerase enzyme complex,[6] suggests that selective and direct targeting of TERRA by small molecules may help to clarify the role of TERRA molecules, especially in protecting telomeres.[46] Targeting of the 3′ single-stranded telomeric DNA overhang by sequestering it into quadruplex DNA is an effective way to inhibit telomerase processivity, with the potential for therapeutic use in human cancers.[17−20] It may then be important to ensure that ligands are able to discriminate between DNA and RNA telomeric quadruplexes, on the basis of their structural features. The distinctive features in the present structure suggest that such discrimination can be achievable. Other types of RNA quadruplexes, especially those derived from untranslated genomic regions, may be amenable targets for artificial regulation of translation under the influence of an RNA quadruplex stabilizing small-molecule ligand.[27−36] The present structure also suggests that such ligands may similarly affect the conformations of the nontelomeric loops in these quadruplexes.

## METHODS

**Crystallization and Data Collection.** The RNA sequence used for crystallization trials, r(UAGGGUUAGGGU), was purchased from Eurogentec (HPLC purified). Synthesis of the triazole-acridine ligand used in these studies has been described previously.[41] Crystals of the complex between the RNA and the triazole-acridine were grown in standard hanging drops. The RNA was annealed at a 1.8 mM single-stranded concentration by heating to 90 °C for 5 min, followed by slow cooling to room temperature overnight in an annealing buffer of 50 mM KCl and 20 mM potassium cacodylate (pH 6.5). RNA and ligand were mixed to final concentrations of 0.75 mM (quadruplex) and 0.5 mM ligand, respectively, and incubated at room temperature for 1 h before mixing with crystallization solution (20% MPD, 150 mM NaCl, 50 mM sodium cacodylate (pH 6.5) and 4 mM spermine). The RNA−ligand complex plus reagent was equilibrated against a well containing 20% MPD at 12 °C, and crystals appeared after 6 weeks. A suitable crystal was screened and characterized on an in-house Oxford Diffraction X-ray machine, and a final data set collected at the U.K. Diamond Light Source synchrotron (beamline I-04). Crystals were found to be in space group *P*23, with cell dimensions and other crystallographic data given in Table 1.

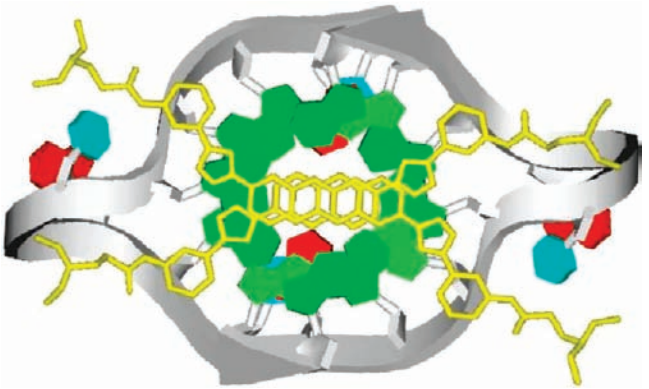

**Figure 5.** Cartoon representation of the crystal structure of the DNA quadruplex−acridine 1:1 complex. The bases in the loops are shown as solid polygons (red for adenine, blue for thymine), and the backbone is shown in ribbon form. A single acridine molecule is shown (as a yellow stick representation) bound on the G-quartet surface as two disordered half-molecules. The sequence crystallized is d(TAGGGTTAGGGT), and crystals of the complex are in the space group $P6_222$ with cell dimensions $a = b = 71.67$, $c = 29.37$ Å. Diffraction data were collected on the U.K. Diamond Light Source, and the structure has been refined to an $R$ of 34.6% for 783 reflections to 3.20 Å resolution. The structure has been deposited (PDB id 3QCR) and will be discussed elsewhere in more detail.

**Data Processing, Structure Solution, and Structure Refinement.** Images were processed and scaled using the d*trek program in the CrystalClear software package (Rigaku Inc.). The structure was solved by molecular replacement using the Phaser program[47] from the CCP4 software package.[48] The native bimolecular RNA quadruplex structure (PDB id 3IBK) was used as a search model, with loop and terminal residues removed. Electron density for the three G-quartets and $K^+$ ions could be clearly seen in the initial $2F_o-F_c$ maps, as well as electron density for the UUA loop and residual density above the 5′ G-quartet into which the ligand core could be accurately placed. The $K^+$ ions were located midway between adjacent G-quartet planes, in bipyramidal prismatic coordination to O6 atoms of the guanine bases. Model building and restrained structure refinement (plus TLS parameters) were performed using Coot[49] and Refmac5.[50] As the phases were improved, the UUA loop could be accurately fitted into electron density, as well as the majority of the ligand (an initial PDB file plus geometric parameters for the ligand was generated using the PRODRG server: http://davapc1.bioch.dundee.ac.uk/prodrg/). Electron density observed beneath the 3′ G-quartet allowed the terminal uracil residues to be placed with reasonable accuracy. Further crystallographic details are given in Table 1.

**Table 1. Crystallographic Data for the Complex[a]**

| | |
|---|---|
| sequence | r(UAGGGUUAGGGU) |
| space group | *P*23 |
| **Unit Cell Dimensions** | |
| *a*, *b*, *c* (Å) | 56.61, 56.61, 56.61 |
| resolution (Å) | 17.90−2.40 |
| $R_{int}$ (%) overall | 5.5 (36.8) |
| $I/\sigma$ | 16.1 (4.3) |
| completeness (%) | 100.0 (100.0) |
| redundancy | 6.6 (6.8) |
| **Refinement** | |
| resolution (Å) | 16.34−2.60 |
| reflections | 1901 |
| $R_{work}/R_{free}$ (%) | 23.6/24.7 |
| no. of atoms | 333 |
| ions | 2 |
| water | 16 |
| overall *B*-factor (Å$^2$) | 26.46 |
| **rms Deviations** | |
| bond lengths (Å) | 0.010 |
| bond angles (deg) | 1.018 |
| PDB ID | 3MIJ |

[a] Values in parentheses refer to the highest resolution shell, 2.49−2.40 Å.

## AUTHOR INFORMATION

**Corresponding Author**
stephen.neidle@pharmacy.ac.uk

## ACKNOWLEDGMENT

We are grateful to CRUK (Programme Grant No. C129/A4489), the EU (FP7 Grant for Molecular Cancer Medicine), and the School of Pharmacy for support. S.S. is a Maplethorpe Fellow of the University of London. This work was carried out with the support of the Diamond Light Source.

## REFERENCES

(1) Blackburn, E. H.; Collins, K. *Cold Spring Harbor Perspect. Biol.* [Online early access]. Doi: 10.1101/cshperspect.a003558. Published Online: July 21, **2010**. http://cshperspectives.cshlp.org/content/early/2010/07/19/cshperspect.a003558.long.
(2) Azzalin, C. M.; Reichenbach, P.; Khoriauli, L.; Giulotto, E.; Lingner, J. *Science* **2007**, *318*, 798–801.
(3) Schoeftner, S.; Blasco, M. A. *Nat. Cell Biol.* **2008**, *10*, 228–236.
(4) Luke, B.; Lingner, J. *EMBO J.* **2009**, *28*, 2503–2510.
(5) Caslini, C.; Connelly, J. A.; Serna, A.; Broccoli, D.; Hess, J. L. *Mol. Cell. Biol.* **2009**, *29*, 4519–4526.
(6) Redon, S.; Reichenbach, P.; Lingner, J. *Nucleic Acids Res.* **2010**, *38*, 5797–5806.
(7) Deng, Z.; Norseen, J.; Wiedmer, A.; Riethman, H.; Lieberman, P. M. *Mol. Cell* **2009**, *35*, 403–413.
(8) Deng, Z.; Campbell, A. E.; Lieberman, P. M. *Cell Cycle* **2010**, *9*, 69–74.
(9) Feuerhahn, S.; Iglesias, N.; Panza, A.; Porro, A.; Lingner, J. *FEBS Lett.* **2010**, *584*, 3812–3818.
(10) Nandakumar, J.; Podell, E. R.; Cech, T. R. *Proc. Natl. Acad. Sci. U.S.A.* **2010**, *107*, 651–656.
(11) Randall, A.; Griffith, J. D. *J. Biol. Chem.* **2009**, *284*, 13980–13986.
(12) Xu, Y.; Kaminaga, K.; Komiyama, M. *J. Am. Chem. Soc.* **2008**, *130*, 11179–11184.
(13) Martadinata, H.; Phan, A. T. *J. Am. Chem. Soc.* **2009**, *131*, 2570–2578.
(14) Phan, A. T. *FEBS J.* **2010**, *277*, 1107–1117.
(15) Parkinson, G. N.; Lee, M. P. H.; Neidle, S. *Nature* **2002**, *417*, 876–880.
(16) Collie, G. W.; Haider, S. M.; Neidle, S.; Parkinson, G. N. *Nucleic Acids Res.* **2010**, *38*, 5569–5580.
(17) Sun, D.; Thompson, B.; Cathers, B. E.; Salazar, M.; Kerwin, S. M.; Trent, J. O.; Jenkins, T. C.; Neidle, S.; Hurley, L. H. *J. Med. Chem.* **1997**, *40*, 2113–2116.
(18) De Cian, A.; Lacroix, L.; Douarre, C.; Temime-Smaali, N.; Trentesaux, C.; Riou, J. F.; Mergny, J.-L. *Biochimie* **2008**, *90*, 131–155.
(19) Burger, A. M.; Dai, F.; Schultes, C. M.; Reszka, A. P.; Moore, M. J.; Double, J. A.; Neidle, S. *Cancer Res.* **2005**, *65*, 1489–1496.
(20) Salvati, E.; Leonetti, C.; Rizzo, A.; Scarsella, M.; Mottolese, M.; Galati, R.; Sperduti, I.; Stevens, M. F. G.; D'Incalci, M.; Blasco, M.; Chiorino, G.; Bauwens, S.; Horard, B.; Gilson, E.; Stoppacciaro, A.; Zupi, G.; Biroccio, A. *J. Clin. Invest.* **2007**, *117*, 3236–3247.
(21) Campbell, N. H.; Parkinson, G. N.; Reszka, A. P.; Neidle, S. *J. Am. Chem. Soc.* **2008**, *130*, 6722–6724.
(22) Campbell, N. H.; Patel, M.; Tofa, A. B.; Ghosh, R.; Parkinson, G. N.; Neidle, S. *Biochemistry* **2009**, *48*, 1675–1680.
(23) Gavathiotis, E.; Heald, R. A.; Stevens, M. F. G.; Searle, M. S. *J. Mol. Biol.* **2003**, *334*, 25–36.
(24) Collie, G.; Reszka, A. P.; Haider, S. M.; Gabelica, V.; Parkinson, G. N.; Neidle, S. *Chem. Commun. (Cambridge, U.K.)* **2009**, 7482–7484.
(25) De Cian, A.; Gros, J.; Guédin, A.; Haddi, M.; Lyonnais, S.; Guittat, L.; Riou, J.-L.; Trentesaux, C.; Saccà, B.; Lacroix, L.; Alberti, P.; Mergny, J.-L. *Nucleic Acids Symp. Ser.* **2008**, 7–8.
(26) Rzuczek, S. G.; Pilch, D. S.; Liu, A.; Liu, L.; LaVoie, E. J.; Rice, J. E. *J. Med. Chem.* **2010**, *53*, 3632–3644.
(27) Kumari, S.; Bugaut, A.; Huppert, J. L.; Balasubramanian, S. *Nat. Chem. Biol.* **2007**, *3*, 218–221.
(28) Huppert, J. L.; Bugaut, A.; Kumari, S.; Balasubramanian, S. *Nucleic Acids Res.* **2008**, *36*, 6260–6268.
(29) Wieland, M.; Hartig, J. S. *Nat. Protoc.* **2009**, *4*, 1632–1640.
(30) Halder, K.; Wieland, M.; Hartig, J. S. *Nucleic Acids Res.* **2009**, *37*, 6811–6817.
(31) Arora, A.; Dutkiewicz, M.; Scaria, V.; Hariharan, M.; Maiti, S.; Kurreck, J. *RNA* **2008**, *14*, 1290–1296.
(32) Morris, M. J.; Basu, S. *Biochemistry* **2009**, *48*, 5313–5319.
(33) Balkwill, G. D.; Derecka, K.; Garner, T. P.; Hodgman, C.; Flint, A. P. F.; Searle, M. S. *Biochemistry* **2009**, *48*, 11487–11495.
(34) Beaudoin, J.; Perreault, J. *Nucleic Acids Res.* **2010**, *38*, 7022–7036.
(35) Gomez, D.; Guédin, A.; Mergny, J.-L.; Salles, B.; Riou, J.-F.; Teulade-Fichou, M.; Calsou, P. *Nucleic Acids Res.* **2010**, *38*, 7187–7198.
(36) Bugaut, A.; Rodriguez, R.; Kumari, S.; Hsu, S. D.; Balasubramanian, S. *Org. Biomol. Chem.* **2010**, *8*, 2771–2776.
(37) Henn, A.; Joachimi, A.; Gonçalves, D. P. N.; Monchaud, D.; Teulade-Fichou, M.; Sanders, J. K. M.; Hartig, J. S. *ChemBioChem* **2008**, *9*, 2722–2729.
(38) Arora, A.; Maiti, S. *J. Phys. Chem. B* **2009**, *113*, 10515–10520.
(39) Joachimi, A.; Benz, A.; Hartig, J. S. *Bioorg. Med. Chem.* **2009**, *17*, 6811–6815.
(40) Xu, Y.; Ishizuka, T.; Kimura, T.; Komiyama, M. A. *J. Am. Chem. Soc.* **2010**, *132*, 7231–7233.
(41) Sparapani, S.; Haider, S. M.; Doria, F.; Gunaratnam, M.; Neidle, S. *J. Am. Chem. Soc.* **2010**, *132*, 12263–12272.
(42) Parkinson, G. N.; Cuenca, F.; Neidle, S. *J. Mol. Biol.* **2008**, *381*, 1145–1156.
(43) Neidle, S.; Parkinson, G. N. *Biochimie* **2008**, *90*, 1184–1196.
(44) Parkinson, G. N.; Ghosh, R.; Neidle, S. *Biochemistry* **2007**, *46*, 2390–2397.

(45) Xu, Y.; Suzuki, Y.; Ito, K.; Komiyama, M. *Proc. Natl. Acad. Sci. U.S.A.* **2010**, *107*, 14579–14584.
(46) de Silanes, I. L.; d'Alcontres, M. S.; Blasco, M. A. *Nat. Commun.* **2010**, *1*, 1–9.
(47) McCoy, A. J.; Grosse-Kunstleve, R. W.; Adams, P. D.; Winn, M. D.; Storoni, L. C.; Read, R. J. *J. Appl. Crystallogr.* **2007**, *40*, 658–674.
(48) Collaborative Computational Project, Number 4: The CCP4 Suite: Programs for Protein Crystallography . *Acta Crystallogr.* **1994**, *D50*, 760−763.
(49) Emsley, P.; Lohkamp, B.; Scott, W. G.; Cowtan, K. *Acta Crystallogr.* **2010**, *D66*, 486–501.
(50) Murshudov, G. N.; Vagin, A. A.; Dodson, E. J. *Acta Crystallogr.* **1997**, *D53*, 240–255.